ISSN 1330-3651(Print), ISSN 1848-6339 (Online)
UDC/UDK 543.55:669.15]:620.197.5

Cr/Fe RATIO BY XPS SPECTRA OF MAGNETOELECTROPOLISHED AISI 316L SS FITTED BY GAUSSIAN-LORENTZIAN SHAPE LINES

Krzysztof Rokosz, Tadeusz Hryniewicz, Steinar Raaen

Original scientific paper

In the paper, the analyses of $Fe2p_{3/2}$ and chromium $Cr2p_{3/2}$ XPS spectra with fitting by symmetrical and asymmetrical line shapes, are presented. The calculations are performed on AISI 316L SS biomaterial after magnetoelectropolishing MEP operation. The best results were obtained for fitting by GL(30) and by LA(1,3; 4; 5) plus GL(40) line shapes. It was found, the chromium-to-iron ratio after magnetoelectropolishing MEP was increasing in the range from 16,4 to 22,4 times versus that one of bulk material.

Keywords: *Cr/Fe ratio, magnetoelectropolishing MEP, 316L stainless steel, XPS spectra fitting*

Omjer Cr/Fe pomoću XPS spektara magnetoelektropoliranog AISI316L SS podešenog Gauss-Lorentzovim oblicima spektralne linije

Izvorni znanstveni članak

U radu su predstavljene analize XPS spektara željeza $Fe2p_{3/2}$ i kroma $Cr2p_{3/2}$ podešavanjem pomoću simetričnih i asimetričnih oblika linija. Izračuni su provedeni na AISI 316L SS biomaterijalu nakon postupka magnetoelektropoliranja MEP. Najbolji rezultati su postignuti za podešavanje pomoću oblika linija GL(30) i LA(1,3; 4; 5) plus GL(40). Ustanovljeno je da se nakon postupka magnetoelektropoliranja MEP omjer kroma i željeza povećao od 16,4 do 22,4 puta u odnosu na onaj u rasutom materijalu.

Ključne riječi: *magnetoelektropoliranje MEP, omjer Cr/Fe, podešavanje XPS spektra, 316L nehrđajući čelik*

1 Introduction

The analyses of XPS spectra after electropolishing in the magnetic field were presented in many previous papers [1 ÷ 8]. Most of them are related to the AISI 316L austenitic stainless steel after magnetoelectropolishing [1, 7 ÷ 10]. In all the papers presented the XPS spectra have been fitted by Gaussian-Lorentzian shape lines. That paper presents and compares the use of various types of line shapes (symmetric and asymmetric) for fitting iron $Fe2p_{3/2}$ and chromium $Cr2p_{3/2}$ XPS spectra.

2 Materials and methods

Stainless steel AISI 316L (S31603, 1.4404) has a good corrosion resistance to general and pitting corrosion, because of its chemical composition. The bulk composition of the steel is shown in Tab. 1. Second column of the Tab. 1 refers to the standard composition, and the third one, as measured. The chromium to iron ratio (Cr/Fe) of that alloy is amounted to 0,25. During a variety of mechanical and/or electrochemical polishing operations the surface layer usually changes considerably. It reveals different chemical composition than that of the matrix, because of the passivation process running during these treatments.

The samples for XPS measurements were treated by Magnetoelectropolishing MEP [9] under definite conditions (B = 400±50 mT, i = 200±20 A/dm^2); after that they were immersed for one year in a Ringer's solution. The polishing was carried out in the electrolyte of temperature of 65 °C, with the temperature control of ±10 °C. For the studies, a proprietary mixed sulfuric/ phosphoric acids electrolyte H_3PO_4/H_2SO_4=1,5 plus 10 % H_2O of the whole acids' volume) was used. The electrolytic cell was made of glass, containing up to 500 cm^3 of electrolyte.

The experiments were carried out in an ultra-high-vacuum system with a base pressure of about 10^{-8} Pa. The XPS measurements, with the angle of 90°, were performed using a SES2002 electron energy analyzer with a monochromatized Al Kα (hν = 1486,6 eV) X-ray source (Gammadata-Scienta). A total resolution of about 0,6 eV was obtained for the presented spectra. In view of optimizing the signal-to-noise ratio, one XPS measurement cycle covered 100 sweeps. For the XPS analyses the CasaXPS 2.3.14 software was used [8, 10 ÷ 13]. The XPS spectra were analysed by using Shirley background.

Table 1 Chemical composition of AISI 316L SS, wt %

Element	Typical composition	Content as measured
Chromium	16 ÷ 18	16,92
Nickel	10 ÷ 14	10,38
Manganese	2 (max)	1,30
Molybdenum	2 ÷ 3	2,01
Nitrogen	0,1 (max)	0,04
Carbon	0,03 (max)	0,02
Silicon	0,75 (max)	0,39
Phosphorus	0,045 (max)	0,32
Sulfur	0,03 (max)	0,01
Copper	-	0,28
Vanadium	-	0,09
Cobalt	-	0,19
Aluminum	-	0,01
Iron	Balance	68,04

For fitting of the XPS spectra the following Gausian-Lorentzian line shapes [13 ÷ 15] were used. The first one of the mathematical formula shown as (1) is the multiplication of the two functions: Gaussian (2) and Lorentzian (3):

$$GL(x:E,F,m)=\frac{e^{-4\ln 2(1-m)\cdot\frac{(x-E)^2}{F^2}}}{1+4m\cdot\frac{(x-E)^2}{F^2}}, \quad (1)$$

$$G(x:E,F,m)=e^{-4\ln 2(1-\frac{m}{4})\cdot\frac{(x-E)^2}{F^2}}, \quad (2)$$

$$L(x:E,F,m)=[1+4m\cdot\frac{(x-E)^2}{F^2}]^{-1}, \quad (3)$$

where the FWHM is related to F and position to E in equations (1)-(3). In Casa XPS the line $GL(x: E, F, m) = GL(m)$, for $m = 0$ represents pure Gaussian one and for $m = 100$ just pure Lorentzian. For the $0 < m < 100$ is obtained mix of the two lines by the formula (1).

The second one (4) is the asymmetric line shape based also on Gausian-Lorentzian shape as:

$$LA(x,\alpha,\beta,F,E)=\begin{cases}[L(x,F,E)]^{\alpha}, & \text{for } x\le E\\ [L(x,F,E)]^{\beta}, & \text{for } x>E\end{cases}. \quad (4)$$

In the Casa XPS the formula is formatted as LA (α, β, m), where $\alpha \neq \beta$ and m is responsible for the control of the width of a Gaussian convolution.

On the basis of the analysis shown in the paper, the authors performed the analysis of the influence of shape lines on the fitting of XPS spectra of $Fe2p_{3/2}$ and $Cr2p_{3/2}$. For this purpose, fittings were done by GL(m=10k), for $k \in N$ and $k<10$, as well as for the metallic part of LA(1,2; 4, 8;3) in case of iron and LA(1,3; 4; 5) for chromium spectra, respectively [15].

3 Results and Discussion

In Tables 2 and 3 there are shown the results of XPS spectra, which are shown in Fig. 1, fitting by other symmetrical and asymmetrical shapes lines. The finding is, that the best fit of $Fe2p_{3/2}$ spectrum has been obtained by LA(1,2; 4,8; 3) for metallic part, and GL(0) for the compounds. In case of the binding energy related to the metallic iron (707,0 ÷ 707,2 eV) the results could not be misinterpreted for all shape lines. However, in case of the compounds fitting line there could be a decision problem.

Table 2 Results of fitting $Fe2p_{3/2}$ data by two peaks

	METAL						COMPOUNDS					RSTD
	Nr	BE / eV	FWHM	L. Sh.	AREA	at %	BE /eV	FWHM	L. Sh.	AREA	at %	-
Surface after Magnetoelectropolishing (MEP 200) 1 year immersion in Ringer's solution	1	707,2	1,30823	GL(0)	17,9	34,94	710,6	4,75392	GL(0)	33,4	65,06	0,0597
	2	707,2	1,30214	GL(10)	18,0	34,98	710,6	4,73661	GL(10)	33,4	65,02	0,0598
	3	707,2	1,30066	GL(20)	18,1	35,27	710,6	4,6786	GL(20)	33,3	64,73	0,0608
	4	707,2	1,29412	GL(30)	18,3	35,54	710,6	4,60674	GL(30)	33,2	64,46	0,0601
	5	707,2	1,28532	GL(40)	18,5	35,86	710,7	4,52092	GL(40)	33,2	64,14	0,0609
	6	707,2	1,27461	GL(50)	18,8	36,23	710,7	4,41692	GL(50)	33,1	63,88	0,0646
	7	707,2	1,26029	GL(60)	19,1	36,64	710,7	4,29878	GL(60)	33,0	63,36	0,0680
	8	707,2	1,2419	GL(70)	19,5	37,15	710,7	4,15144	GL(70)	32,9	62,85	0,0732
	9	707,2	1,21814	GL(80)	20,0	37,87	710,8	3,95736	GL(80)	32,8	62,13	0,0813
	10	707,2	1,18083	GL(90)	20,8	38,82	710,8	3,71833	GL(90)	32,9	61,18	0,0949
	11	707,2	1,12375	GL(100)	25,2	41,50	710,9	3,33729	GL(100)	35,5	58,50	0,1224
	12	707,2	1,35009	GL(0)	18,3	30,76	710,7	3,69809	GL(100)	41,3	69,24	0,1011
	13	707,2	1,11248	GL(100)	25,5	46,78	710,8	4,39317	GL(0)	29,0	53,22	0,0850
	14	**707,0**	**0,929887**	**LA(1,2;4,8;3)**	**27,4**	**53,76**	**711,2**	**3,72428**	**GL(0)**	**23,6**	**46,24**	**0,0493**
	15	707,0	0,927923	LA(1,2;4,8;3)	27,3	53,54	711,2	3,7293	GL(10)	23,7	46,46	0,0494
	16	707,0	0,927123	LA(1,2;4,8;3)	27,3	53,36	711,1	3,70746	GL(20)	23,8	46,64	0,0495
	17	707,0	0,923743	LA(1,2;4,8;3)	27,1	53,00	711,1	3,69611	GL(30)	24,0	47,00	0,0498
	18	707,0	0,91861	LA(1,2;4,8;3)	26,9	52,50	711,1	3,67722	GL(40)	24,3	47,50	0,0502
	19	707,0	0,915809	LA(1,2;4,8;3)	26,7	52,08	711,1	3,63635	GL(50)	24,6	47,92	0,0507
	20	707,0	0,911264	LA(1,2;4,8;3)	26,5	51,45	711,1	3,60761	GL(60)	25,0	48,55	0,0515
	21	707,0	0,905765	LA(1,2;4,8;3)	26,2	50,72	711,1	3,5578	GL(70)	25,4	49,28	0,0527
	22	707,0	0,900476	LA(1,2;4,8;3)	25,9	49,83	711,1	3,48395	GL(80)	26,1	50,17	0,0548
	23	707,0	0,896434	LA(1,2;4,8;3)	25,6	48,68	711,1	3,36066	GL(90)	27,0	51,32	0,0588
	24	707,0	0,897811	LA(1,2;4,8;3)	25,4	44,43	711,0	3,12920	GL(100)	31,7	55,57	0,0684
Mean	**707,1**		**1,096141**	-	**22,9**	**43,57**	**710,9**	**3,94075**	-	**29,8**	**56,43**	**0,0657**
Minimum	**707,0**		**0,896434**	-	**17,9**	**30,76**	**710,6**	**3,1292**	-	**23,6**	**46,24**	**0,0493**
Maximum	**707,2**		**1,35009**	-	**27,4**	**53,76**	**711,2**	**4,75392**	-	**41,3**	**69,24**	**0,1224**
Std. dev.	**0,1**		**0,179133**	-	**3,9**	**7,9**	**0,2**	**0,49014**	-	**4,9**	**7,91**	**0,0189**

Table 3 Results of fitting $Cr2p_{3/2}$ data by two peaks

	METAL						COMPOUNDS					RSTD
	Nr	BE / eV	FWHM	L. Sh.	AREA	at %	BE / eV	FWHM	L. Sh.	AREA	at %	-
Surface after Magnetoelectropolishing (MEP 200) 1 year immersion in Ringer's solution	1	574	1,03928	GL(0)	4,6	4,53	577,0	2,88769	GL(0)	96,4	95.,47	0,0780
	2	574	1,02973	GL(10)	4,5	4,44	577,0	2,88123	GL(10)	96,5	95,56	0,0764
	3	574	1,00689	GL(20)	4,3	4,25	577,0	2,86468	GL(20)	96,9	95,75	0,0737
	4	**574**	**0,968778**	**GL(30)**	**4,0**	**3,95**	**577,0**	**2,8432**	**GL(30)**	**97,4**	**96,05**	**0,0720**
	5	574	0,927658	GL(40)	3,7	3,63	577,0	2,81638	GL(40)	98,0	96,37	0,0729
	6	574	0,876692	GL(50)	3,3	3,25	577,0	2,78289	GL(50)	98,8	96,75	0,0782
	7	574	0,800334	GL(60)	2,9	2,78	577,0	2,74344	GL(60)	99,8	97,22	0,0899
	8	574	0,719331	GL(70)	2,3	2,27	577,0	2,69124	GL(70)	101,0	97,73	0,1100
	9	574	0,630179	GL(80)	1,9	1,81	577,0	2,61262	GL(80)	102,6	98,19	0,1417
	10	574,3	1,13303	GL(90)	4,6	4,81	577,0	2,36952	GL(90)	91,1	95,19	0,2646
	11	574	0,747704	GL(100)	3,1	2,78	577,0	2,15733	GL(100)	107,9	97,22	0,4231
	12	574	0,885631	GL(0)	6,1	6,03	577,0	2,87373	GL(100)	95,6	93,97	0,0903
	13	574	0,88372	GL(100)	6,2	6,08	577,0	2,86941	GL(0)	95,5	93,92	0,0902
	14	573,8	0,72675	LA(1,3;4;5)	5,6	5,54	577,0	2,86435	GL(0)	95,3	94,46	0,0901
	15	573,8	0,71661	LA(1,3;4;5)	5,5	5,41	577,0	2,85879	GL(10)	95,5	94,59	0,0885
	16	573,8	0,703931	LA(1,3;4;5)	5,2	5,11	577,0	2,8445	GL(20)	94,89	95,90	0,0853
	17	573,8	0,674214	LA(1,3;4;5)	4,7	4,69	577,0	2,82613	GL(30)	96,6	95,31	0,0827
	18	573,8	0,646906	LA(1,3;4;5)	4,3	4,26	577,0	2,80166	GL(40)	97,3	95,74	0,0822
	19	573,8	0,612431	LA(1,3;4;5)	3,8	3,74	577,0	2,77178	GL(50)	98,2	96,26	0,0855
	20	573,8	0,573172	LA(1,3;4;5)	3,3	3,18	577,0	2,73284	GL(60)	99,3	96,82	0,0945
	21	573,8	0,535103	LA(1,3;4;5)	2,7	2,58	577,0	2,68331	GL(70)	100,7	97,42	0,1123
	22	573,8	0,477042	LA(1,3;4;5)	2,0	1,93	577,0	2,6159	GL(80)	102,6	98,07	0,1428
	23	573,8	0,383191	LA(1,3;4;5)	1,2	1,13	577,0	2,5073	GL(90)	105,6	98,87	0,1949
	24	573,8	0,803241	LA(1,3;4;5)	2,9	2,65	577,0	2,17082	GL(100)	106,2	97,35	0,3799
Mean		**573,9**	**0,770898**	-	**3,9**	**3,78**	577,0	**2,71128**	-	**98,7**	**96,25**	**0,1292**
Minimum		**573,8**	**0,383191**	-	**1,2**	**1,13**	577,0	**2,15733**	-	**91,1**	**93,92**	**0,0720**
Maximum		**574,3**	**1,13303**	-	**6,2**	**6,08**	577,0	**2,88769**	-	**107,9**	**98,87**	**0,4231**
Std. dev.		**0,1**	**0,191352**	-	**1,3**	**1,37**	**0**	**0,212167**	-	**3,9**	**1,34**	**0,0950**

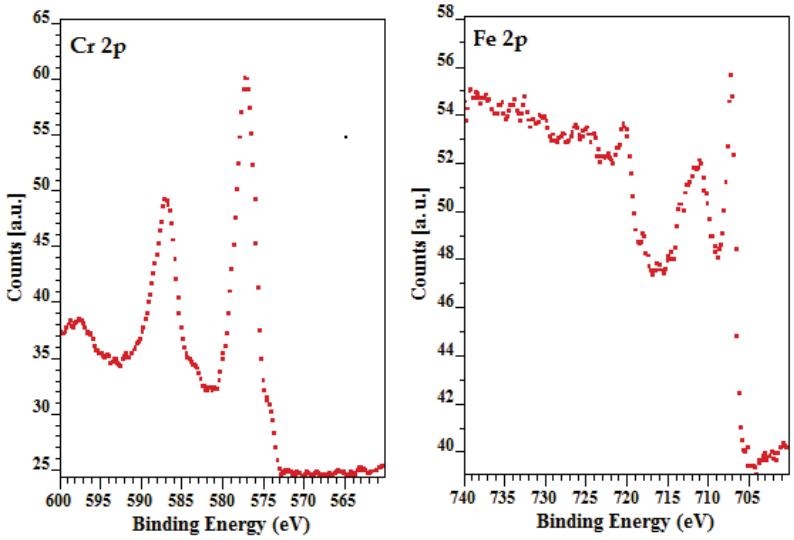

Figure 1 XPS high resolution results of Cr2p and Fe2p spectra of AISI 316L SS after MEP

Fitting by two peaks is not the best method, but with well-chosen line shapes it should provide essential information about the predominance of oxides, hydroxides as well as phosphates and sulfates of iron. It should be taken into account that the alloy consists of 14 chemical elements, which form compounds with each

other. A lot of peaks with the same binding energy relate to the other chemicals compounds, e.g. $FeSO_4$, Fe^{2+} (711,0 ÷ 712,2 eV) and FeOOH, Fe^{3+} (710,2 ÷ 711,8 eV). If there is a pure chemical iron compound, then it is rather easy to assess the oxide states of iron; on the other hand, in case of alloy such as AISI 316L SS, the task is much more difficult. In that case in the passive layer the compounds of iron or other complex compounds such as iron-chromium-nickel- molybdenum with oxygen, sulfur and phosphorus, can be detected. In that situation the best solution is to separate metal and compounds' parts.

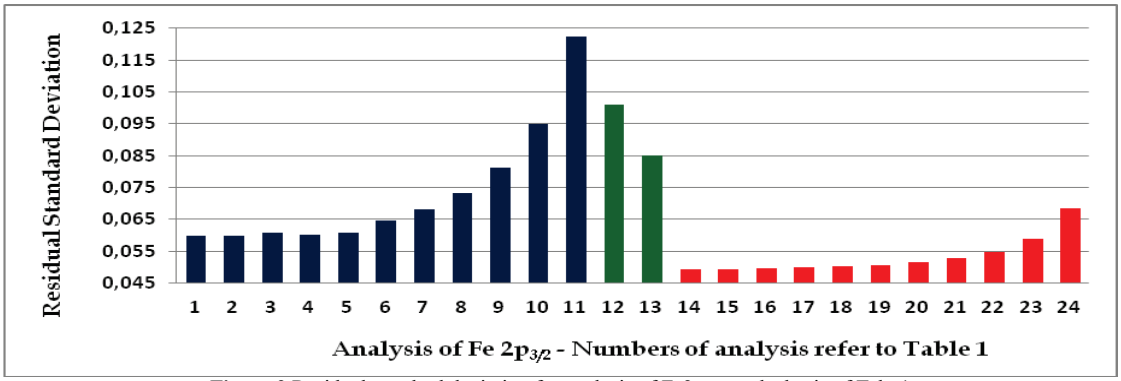

Figure 2 Residual standard deviation for analysis of $Fe2p_{3/2}$ on the basis of Tab. 1

Table 4 Results of Cr/Fe ratio

Nr	RSTD(Fe)	RSTD(Cr)	RSTD(Fe) + RSTD(Cr)	Cr-M/Fe-M	Cr-X/Fe-X
1	0,0597	0,0780	0,1377	0,4	4,0
2	0,0598	0,0764	0,1362	0,4	4,0
3	0,0608	0,0737	0,1345	0,3	4,1
4	**0,0601**	**0,0720**	0,1321	**0,3**	**4,1**
5	0,0609	0,0729	0,1338	0,3	4,1
6	0,0646	0,0782	0,1428	0,2	4,2
7	0,0680	0,0899	0,1579	0,2	4,2
8	0,0732	0,1100	0,1832	0,2	4,3
9	0,0813	0,1417	0,2230	0,1	4,4
10	0,0949	0,2646	0,3595	0,3	3,9
11	0,1224	0,4231	0,5455	0,2	4,3
12	0,1011	0,0903	0,1914	0,5	3,2
13	0,0850	0,0902	0,1752	0,3	4,6
14	**0,0493**	**0,0901**	**0,1394**	**0,3**	**5,7**
15	0,0494	0,0885	0,1379	0,3	5,6
16	0,0495	0,0853	0,1348	0,3	5,6
17	0,0498	0,0827	0,1325	0,2	5,6
18	**0,0502**	**0,0822**	**0,1324**	**0,2**	**5,6**
19	0,0507	0,0855	0,1362	0,2	5,6
20	0,0515	0,0945	0,146	0,2	5,6
21	0,0527	0,1123	0,165	0,1	5,6
22	0,0548	0,1428	0,1976	0,1	5,5
23	0,0588	0,1949	0,2537	0,1	5,5
24	0,0684	0,3799	0,4483	0,2	4,7
		Mean		0,2	4,8
		Minimum		0,1	3,2
		Maximum		0,5	5,7
		Standard deviation		0,1	0,8

Results of fitting $Fe2p_{3/2}$ data by two-peak analysis are given in Tab. 2. The minimal errors (Fig. 1) of the XPS data analysis, presented in Tab. 2, are observed for fitting metal part by LA(1,2; 4,8; 3) and compounds part by GL(m=0, 10, 20). In case of the binding energy differences for metal part the deviation is so small that it is not possible to misinterpret the iron as a metal. For iron compounds fitted by GL(m=10k), for $k \in N$ and k<10 lines, the range of data is only 0,2 eV (710,6 ÷ 710,8 eV), which may clearly indicate the predominance of Fe_2O_3, Fe^{3+} [14 ÷ 20]. However, this method provides the possibility to investigate significant differences between the obtained XPS spectra. On the other hand, the XPS fitted by LA(1,2; 4,8; 3) and GL(m=10k), for $k \in N$ and k<10, have been pointed to other chemical compounds, i.e. FeOOH, Fe^{3+} (711,0 ÷ 711,2 eV) [14 ÷ 20]. The most important finding is that the whole proceeding algorithm must be shown and at the end a proposal of the most probable chemical compounds (here Fe_2O_3/ FeOOH), with a focus on oxidation stage (here Fe^{3+}) should be given. In Tab. 3 and Fig. 3 there are shown the residual standard deviations of iron and chromium separately and as a sum, as well as chromium metal/compounds to iron metal/compounds Cr-M/Fe-M and Cr-X/Fe-X ratios. There is visible, that the best fitting of XPS $Fe2p_{3/2}$ and $Cr2p_{3/2}$ is observed for GL(30) (position 4 in Tab. 3) line

and LA(1,3; 4; 5), GL(40) (position 18 in Tab. 3). In these points the Cr-X/Fe-X are different. The difference amounts to 1,5. The authors recommend to present the result as the interval, as the most authoritative description of passive layers formed after magnetoelectropolishing MEP, here Cr-X/Fe-X∈<4,1; 5,6>.

In case of chromium spectra (Tab. 2) there is no problem with identification of the chemical compounds. For all fitting lines the results of chromium metal and compounds are obviously: 573,8 ÷ 574,0 eV, what corresponds to the chromium metal and 577,0 eV to CrOOH, Cr^{3+} [14 ÷ 17]. The minimal fitting error is observed for using GL(30) to the metallic part as well as to compounds part of XPS spectrum (Fig. 2).

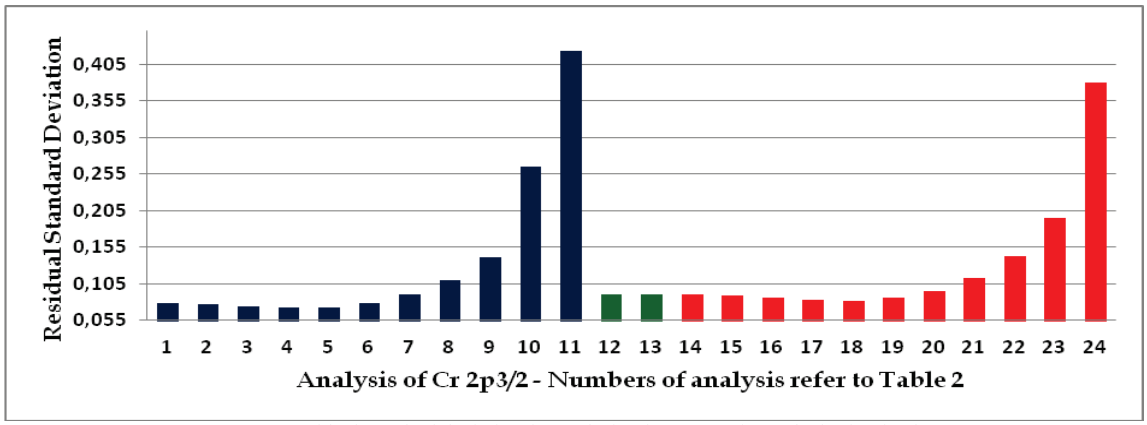

Figure 3 Residual standard deviation for analysis of $Cr2p_{3/2}$ ratio on the basis of Tab. 3

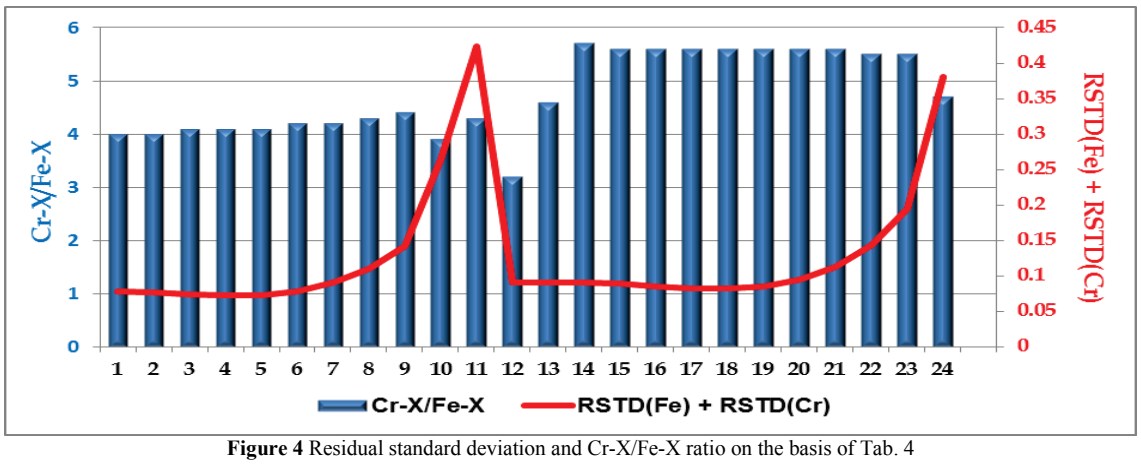

Figure 4 Residual standard deviation and Cr-X/Fe-X ratio on the basis of Tab. 4

4 Conclusion

In the paper there are presented the analyses of $Fe2p_{3/2}$ and chromium $Cr2p_{3/2}$ XPS spectra with fitting by symmetrical and asymmetrical line shapes. Authors decided using Gaussian-Lorentzian shape lines: GL(m=10k), for $k \in N$ and k<10, as well as for LA(1,2; 4,8; 3) and LA(1,3; 4; 5). The results have shown that the best outcomes were obtained for chromium and iron fitting by GL(30) lines as well as chromium by LA(1,3; 4; 5) (metal) plus GL(40) (compounds) and iron by LA(1,2; 4,8; 3) (metal) plus GL(40) (compounds) line shapes. The calculated Cr-X/Fe-X ratio is in the range closed from 4,1 to 5,6, that means the significant improvement of surface layer passivity versus that one calculated from the matrix composition, i.e. amounting to 0,25 (see Tab. 1), is obtained. In summary of the discussion, it is important to focus on the fact that the chromium-to-iron ratio after Magnetoelectropolishing MEP is increasing in the range from 16,4 to 22,4 times versus that one of bulk material.

5 References

[1] Rokosz, K. Polerowanie elektrochemiczne stali w polu magnetycznym (Electrochemical polishing of steels in magnetic field), Monograph nr 219, Publisher: Koszalin University of Technology, Koszalin, ISSN 0239-7129, 211 pages – (in Polish), 2012.

[2] Hryniewicz, T.; Rokicki, R.; Rokosz K. Magnetoelectropolishing for metal surface modification. // Transactions of the Institute of Metal Finishing. 85, 6(2007), pp. 325-332.

[3] Hryniewicz, T.; Rokicki, R.; Rokosz K. Surface characterization of AISI 316L biomaterials obtained by electropolishing in a magnetic field. // Surface and Coatings Technology. 202, 9(2008), pp. 1668-1673.

[4] Hryniewicz, T.; Rokosz, K.; Rokicki, R. Electrochemical and XPS Studies of AISI 316L Stainless Steel after Electropolishing in a Magnetic Field. // Corrosion Science. 50, 9(2008), pp. 2676-2681.

[5] Hryniewicz, T.; Rokicki, R.; Rokosz, K. Corrosion Characteristics of Medical Grade AISI 316L Stainless Steel Surface after Electropolishing in a Magnetic Field. // CORROSION (The Journal of Science and Engineering), Corrosion Science Section. 64, 8(2008), pp. 660-665.

[6] Hryniewicz, T.; Rokosz, K. Polarization Characteristics of Magnetoelectropolishing Stainless Steels. // Materials Chemistry and Physics. 122, 1(2010), pp. 169-174.
[7] Hryniewicz, T.; Rokosz, K. Analysis of XPS results of AISI 316L SS electropolished and magnetoelectropolished at varying conditions. // Surface and Coatings Technology. 204, 16-17(2010), pp. 2583-2592.
[8] Rokosz, K.; Hryniewicz, T.; Raaen, S. Characterization of Passive Film Formed on AISI 316L Stainless Steel after Magnetoelectropolishing in a Broad Range of Polarization Parameters. // Steel Research International. 83, 9(2012), pp. 910-918.
[9] Rokicki, R. US Patent No 7632390, http://www.patentgenius.com/patent/7632390.html
[10] Hryniewicz, T.; Rokosz, R. Investigation of selected surface properties of AISI 316L SS after magnetoelectropolishing. // Materials Chemistry and Physics. 123, (2010), pp. 47-55. DOI: 10.1016/j.matchemphys.2010.03.060
[11] Fairley, N. http://www.casaxps.com, © Casa software Ltd. 2005.
[12] Walton, J.; Carrick, A. The Casa Cookbook-The CasaXPS User's Manual, Part 1: Recipes for XPS data proceedings. ISBN: 9780954953300, Publisher: Acolyte Science, 2009.
[13] CasaXPS Processing Software, CasaXPS Manual 2.3.15 Rev 1.0, Copyright © Casa Software Ltd, 19-20, 2010.
[14] Biesinger, M. C.; Payne, B. P.; Grosvenor, A. P.; Lau L. W. M.; Gerson, A. R.; Smart, R. St. C. Resolving surface chemical states in XPS analysis of first row transmition metals, oxides and hydrooxides: Cr, Mn, Fe, Co and Ni. // Applied Surface Science. 257 (2011), pp. 2717-2730.
[15] Crist, B. V. Handbook of monochromatic XPS spectra, The elements and native oxides. John Wiley & Sons, Ltd., 2000.
[16] Moulder, J. F.; Stickle, W. F.; Stickle, Sobol P. E.; Bomben, K. D. Handbook of X-ray Photoelectron Spectroscopy, A Reference Book of Standard Spectra for Identification and Interpretation of XPS Data. Perkin-Elmer Corporation, 1992.
[17] Tauson, V. L.; Kravtsova, R. G.; Grebenshchikova, V. I.; Lustenberg, E. E.; Lipko, S. V. Surface typochemistry of hydrothermal pyrite: Electron spectroscopic and scanning probe microscopic data. I. Synthetic pyrite. // Geochemistry International. 48, 6(2010), pp. 565-577.
[18] Descostes, M.; Mercier, F.; Thromat, N.; Beaucaire, C.; Gautier-Soyer, M. Use of XPS in the determination of chemical environment and oxidation state of iron and sulfur samples: constitution of a data basis in binding energies for Fe and S reference compounds and applications to the evidence of surface species of an oxidized pyrite in a carbonate medium. // Applied Surface Science. 165 (2000), pp. 288–302.
[19] Fantauzzi, M.; Pacella, A.; Atzei, D.; Gianfagna, A.; Andreozzi, G.,B.; Rossi, A. Combined use of X-ray photoelectron and Mössbauer spectroscopic techniques in the analytical characterization of iron oxidation state in amphibole asbestos. // Analytical and Bioanalytical Chemistry. 396, 8(2010), pp. 2889-2898.
[20] Grosvenor, A. P.; Kobe, B. A.; Biesinger, M. C.; McIntyre, N. S. Investigation of multiplet splitting of Fe 2p XPS spectra and bonding in iron compounds. // Surface and Interface Analysis. 36 (2004), pp. 1564-1574.

Authors' addresses

Krzysztof Rokosz
Faculty of Mechanical Engineering
Koszalin University of Technology
Racławicka 15-17, 75-620 Koszalin
Poland
E-mail: rokosz@tu.koszalin.pl

Tadeusz Hryniewicz *(corresponding author)*
Faculty of Mechanical Engineering
Koszalin University of Technology
Racławicka 15-17, 75-620 Koszalin
Poland
E-mail: Tadeusz.Hryniewicz@tu.koszalin.pl

Steinar Raaen
Physics Departament
NTNU, NO-7491 Trondheim
Norway
E-mail: sraaen@ntnu.no